Active Search methods to predict material failure under intermittent loading in the Serebrinksy-Ortiz fatigue model

Stephen Guth[1] and Themistoklis Sapis[1]

Massachusetts Institute of Technology, Cambridge, MA 02139, USA,
tsapsis@mit.edu,
home page: http://sandlab.mit.edu/

Abstract. The rainflow counting algorithm for material fatigue is both simple to implement and extraordinarily successful for predicting material failure times. However, it neglects memory effects and time-ordering dependence, and therefor runs into difficulties dealing with intermittent loads, especially those with long tailed distributions. In this report, we use the Serebrinsky-Ortiz model of material fatigue to introduce a partial analytical solution for deterministic intermittent loads, which greatly improves integration speed while still conservatively identifying early failures. Additionally, we apply recent advances in optimal experimental design both to gain insight into how rare events lead to extreme early material failure, and to estimate the long tail of the distribution of failure times.

Keywords: Fatigue · Rare events · Extreme events · Intermittent events · Active search · Optimal experimental design

1 Introduction

The modern energy industry increasingly relies on enormously capital intensive structures, which are placed in extreme conditions and subject to extreme loads that vary throughout the structure's expected lifetime. Failure costs are astronomical, including forgone profits, legal penalties, tort payouts, and reputation damage [9]. Minimizing lifetime costs require safe-life engineering and a conservative assessment of failure probabilities. Unfortunately, while material fatigue is a major contributor to failure, non destructively measuring fatigue is both difficult and expensive [25].

For many classes of structure, fatigue loads have important intermittent stochastic character [1][10][24]. In particular, traditional frequency domain approaches have difficulty predicting the fatigue lifetime effects of intermittent loading, which have important dependence on time-ordering.

A major limitation to simulating the effects of intermittent loading is the time cost of Monte Carlo simulations, which grows quickly in the dimension of the search space. Alternative approaches include statistical linearization [22][17][6], hierarchical modeling [26][18], structured sampling methods [19], and optimal experimental design [2][15][23][11][13].

In this work, we will develop a computational scheme for the fatigue model developed by Serebrinksy and Ortiz with important time-ordering effects. To speed computation, we will develop an analytical method based on both statistical linearization and domain decomposition into quiescent and extreme load increments. This method will allow for efficiently computing the failure time for deterministic intermittent loads. Finally, we will show how an appropriately designed active search scheme can capture the long tail behavior of early fatigue failure with only a small number of numerical experiments.

2 Analytical Method for Deterministic Load

2.1 Serebrinsky-Ortiz Model

Consider a single finite element with one dimensional linear loading. The applied load (stress) is a continuous random process given by $\sigma(t;\omega)$ and the corresponding strain $\delta(t;\omega)$ depends on the element's constitutive relation. The argument for this random process are $t \in [0, T_{max}]$, the time variable and $\omega \in \Omega$, an element from the probability space (i.e., the random argument). Further, this constitutive relation depends on the fatigue state of the material; after some number of loading/unloading cycles N_{fail}, the material stiffness will degrade and eventually the material will fail. Our interest is in the relationship between the load $\sigma(t;\omega)$ and the failure time N_{fail}.

The Serebrinsky-Ortiz model, detailed in Serebrinksy, et al (2005) [21][12], is a constitutive relationship between applied stress, σ, material strain, δ, and material stiffness parameters K^+ and K^-, given by

$$\dot{\sigma} = \begin{cases} K^- \dot{\delta} & \dot{\delta} < 0 \\ K^+ \dot{\delta} & \dot{\delta} > 0 \end{cases} \tag{1}$$

$$\dot{K}^+ = \begin{cases} (K^+ + K^-)\frac{\dot{\delta}}{\delta_a} & \dot{\delta} < 0 \\ -K^+ \frac{\dot{\delta}}{\delta_a} & \dot{\delta} > 0 \end{cases} \tag{2}$$

where δ_a is the fatigue endurance length.

In particular, K^- is assumed to be constant during unloading. These equations model fatigue-crack nucleation and growth via loading-unloading hysteresis. Critical material failure occurs when the parametric stress-strain curve $(\delta(t), \sigma(t))$ crosses a certain coherent envelope.

An example form for the coherent envelope is described by the uber relation

$$\sigma^* = e\sigma_c \frac{\delta}{\delta_c} \exp -\frac{\delta}{\delta_c}, \tag{3}$$

with constants δ_c, σ_c characterizing the material and constant $e \approx 2.718$.

This cohesive envelope has an ascending limb (approximately $\delta < \delta_c$) and a descending limb (approximately $\delta > \delta_c$). If the stress-strain curve crosses the ascending limb, material fatigue accumulates discontinuously, and δ jumps (if possible) to say under the cohesive envelope. If the stress-strain curve crosses in the descending limb, however, there is no greater value of δ, and the material fails.

Equations 2 may be integrated between two local maxima σ_n^+ and σ_{n+1}^+ to give the update rule:

$$K_n^+ = K_n^- - \exp(\frac{\Delta\sigma_n^-}{\delta_a K_n^-})(K_n^- - K_{n-1}^+) - \frac{\Delta\sigma_n^+}{\delta_a}. \tag{4}$$

Figure 1 (b) exhibits a clear linear regime in which the evolution of K^+ satisfies a simple linear relationship:

$$K_n^+ - K_{n-1}^+ \approx \Delta K. \tag{5}$$

The remaining regions, corresponding to the discontinuous jumps in figure 1 (b), correspond to intersections of the (σ, δ) curve with the coherent envelope. This breakdown of an intermittent

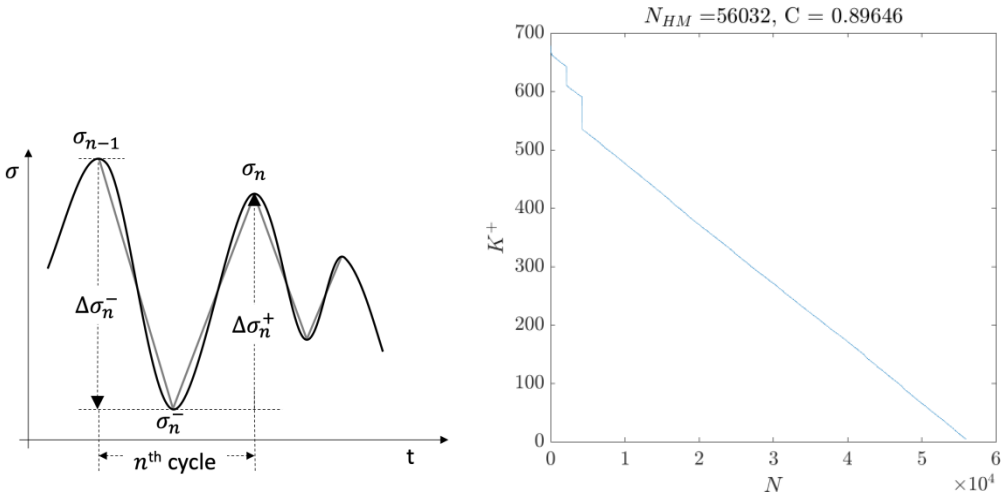

Fig. 1: a) Illustration of the linear approximation $\Delta\sigma_n^{\pm}$, derived from $\sigma(t)$. b) Sample time evolution of K^+ for the Serebrinsky-Ortiz model, for an intermittent load signal. Note the two discontinuous jumps near $t = 0.25 \times 10^4$ and $t = 0.5 \times 10^4$, which correspond to intersections with the ascending leg of the coherent envelope.

process into a linear region and an extreme region parallels the probabilistic decomposition framework developed by Mohamad and Sapsis (2015)[16] and others [14].

In order to use this approximate analytical algorithm, we will require an estimate of the stiffness slope ΔK, the mean change in K^+ per loading/unloading cycle. To find ΔK, we merely need to consult the graph in figure 1, and estimate the slope of the linear regions. This approach requires access to the time history of K^+ during an experiment or numerical simulation.

Alternately, an analytical estimate for ΔK may be obtained by combining the statistics of the load process (via a Rice-type formula) with a linearization of equation 4.

Taken together, equations 4 and 5, along with a rule that identifies local maxima that may potentially intersect the coherent envelope, represent an algorithm for identifying the failure time of a material subject to a known load signal. This algorithm can be run on consumer desktop hardware in seconds–the major speed bottleneck is running the heuristic which filters out local maxima which are unlikely lead to intersections with the coherent envelope.

2.2 Comparison to Palmgren-Miner Rule

A simple method to compute the fatigue effects of intermittent signals is the Palmgren–Miner Rule, given by

$$\sum_i \frac{n_i}{N_{fi}} = C, \tag{6}$$

where n_i is the number of cycles with amplitude corresponding to bin i, and N_{fi} is the number of cycles until failure corresponding to harmonic loading with the same amplitude. This method allows for calculation of equivalent fatigue by breaking the load signal into individual cycles, each of whose

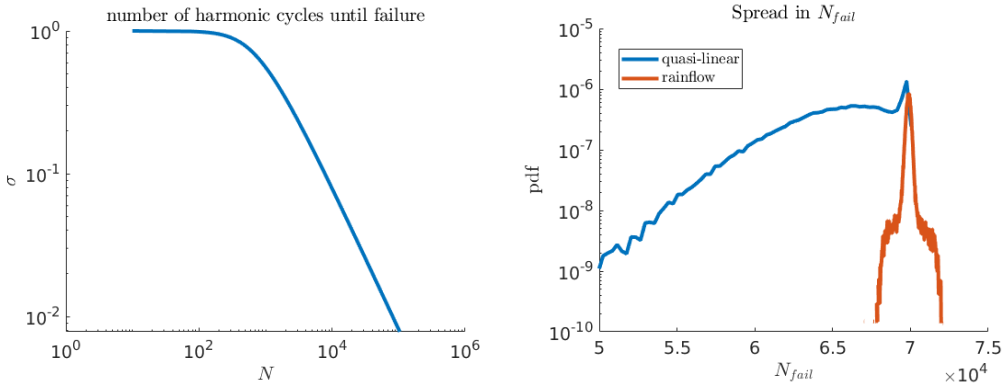

Fig. 2: a) Sample SN plot for the Serebrinksy-Ortiz fatigue model with uber coherent envelope. b) Comparison of the distribution of error times between the analytic model and rainflow counting. The full integration pdf overlaps the analytic model completely. Note that rainflow counting fails to capture the long left tail.

contributions is separately determined by reference to the SN-Curve [7]. The well known rainflow counting algorithm, developed by Endo and Matsuishi [8], implements this rule by breaking a given signal into the corresponding set of increments.

Figure 2 (b) shows the relative errors introduced by approximating the Serebrinsky-Ortiz fatigue model by the rainflow counting method and by the analytical threshold-slope approximation. While both methods predict the mode of the distribution well, rainflow counting substantially underestimates the variance–in particular by discounting the early failure times associated with the long left tail.

3 Output-Weighted Optimal Experimental Design

3.1 Overview

We will address two primary goals for fatigue modeling. First, for a given distribution of load signals, we would like to estimate the distribution of N_{fail}, $f_N(n)$, especially the long tail of early failures. Second, we would like to identify certain characteristics of the load signals that lead to early failure–that is, we would like to identify early failure precursors.

If we had access to an exact expression for the material's coherent envelope, we could compute a distribution of failure times analytically, by finding the joint pdf of ascending and descending leg intersections and marginalizing for the failure time pdf. While this approach gives the advantage of easy updates if the coherent envelope or load statistics are changed, it has the disadvantage of requiring a very accurate estimate of the material's coherent envelope, an abstract function that is difficult to measure directly.

Instead, we will attempt to estimate the failure time pdf directly by performing (numerical) experiments. This will serve two purposes. First, the experimental design suggested will be (somewhat) agnostic to the underlying theoretical model; that is to say, the experimental design will be robust to some model mispecification. Second, assuming that the Serebrinsky-Ortiz model is a good fit for

the material fatigue lifetime, the proposed experimental design will also allow for an estimation of the coherent envelope.

Standard Monte Carlo techniques for estimating probability density functions (pdfs) will require a large number of simulations, each of which is expensive even with the analytical approximation. Instead, we will use a active search methodology that accurately models the long tail of the distribution $f_N(n)$ without a large number of experiments.

3.2 *J*-Spike Model

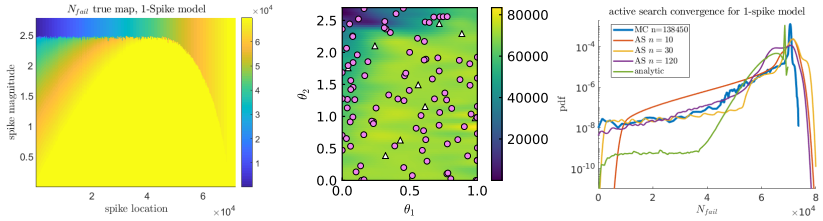

Fig. 3: a) Failure time of the 1-spike model, for different values of spike magnitude and location. b) Graphical representation of surrogate model after 104 black box evaluations. c) Sample pdf of surrogate function derived from active search with Q criterion goal, compared against Monte Carlo simulation of the 1-spike model.

It will be useful to define a class of intermittent signals called the J-spike model, which take the form

$$\sigma^J(t) = B + \sum_i^p a_i \cos(\omega_i t + \phi_i) + \sum_j \alpha_j^J G(t - \beta_j T_{max}) \tag{7}$$

This signal may be broken into a DC offset term, a narrowbanded background sum of sinusoids, and J distinct localized spikes with shape $G(t)$. We will assume that $G(t)$ is unimodal, and has small width relative to the characteristic background wavelength. Further, we will assume that the β_j and α_j are random variables drawn, respectively, from a uniform distribution, and a hand-turned Rayleigh distribution.

Note that for fixed J, the J-spike model does *not* satisfy the independent spike hypothesis.

3.3 Problem Setup

Let us consider the J-spike model described above in section 3.2, restricted to the case $J = 1$. This is a space of signals with two parameters: the location of the spike α_1, and the magnitude of the spike β_1. We will let α_1 be drawn uniformly on the range $[0, 7.2e4]$ (slightly longer than the background failure time), and let β_1 be drawn from the Rayleigh distribution with tuned scale parameter. This scale parameter is tune so that few signals will have a maximum load that exceeds σ_c, but many signals will have one peak that reaches an appreciable fraction of σ_c.

Figure 3 shows the true map from the parametrized 1-spike signal to N_{fail}. This map clearly shows how both the magnitude and time-history of an intermittent load spike work together to affect the material failure time N_{fail}.

We will use use the Gaussian Process package developed by Blanchard and Sapis [3][4] to construct a surrogate function $\tilde{N}(\alpha_1, \beta_1)$ so that for corresponding stress signals, $\tilde{N} \approx N_{fail}$.

Briefly, at each step the algorithm will create an intermediate surrogate model $\tilde{N}^i$ with Gaussian Mixture Model (GMM) form. It will then choose a parameter pair $x = (\alpha_1, \beta_1)$ by minimizing the Q-criterion, developed by Themistoklis Sapsis [20] and given by

$$Q[\sigma_N^2] = \int \frac{p_x(x)}{p_{N_0}(N_0(x))} \sigma_N^2(x; h) dx. \tag{8}$$

Finally, the algorithm will simulate the fatigue lifetime of the material using the chosen parameters, and update the surrogate model.

Unlike the Kullbeck-Liebler divergence, which selects experiments to maximum mutual information with the surrogate [5], the Q-criterion attempts to minimize the variance of the surrogate model along its entire support. In particular, this causes the Q-criterion to reduce the uncertainty in the tails of the surrogate model faster than other information theoretic metrics.

Finally, in order to simulate the scenario where we are cost limited by the difficulty of physical experiments, we will focus on small $n < 100$ simulations. Therefore, will should not expect to fit the map in figure 3 perfectly. Instead, we will seek to make a qualitative fit that matches a few of the major features, and the long tail behavior of the derived failure time pdf.

To this end, we will consider three error metrics. First, we will compare the recovered pdf to a high quality pdf generated by a Monte Carlo sampling strategy with $N = 138450$ samples. Unfortunately, typical error norms such as l_2 or KL divergence will overemphasize errors in the mode of the distribution, to the exclusion of fitting the long tail. To address with, we will also consider a 'tail mass' error metric, which compares the true mass and the recovered mass of the pdf long tail past some fixed threshold. Finally, we will compare the error between the recovered GMM map and the true map (constructed via careful grid sampling). While we shouldn't except close agreement (due to the issues mentioned above), a qualitative match for the recovered map is important to our subgoal of describing the particular load sequences that lead to early material failures.

3.4 Results

Figure 3 shows the evolution of the surrogate pdf trained on 1-spike model signals as the number of samples increases, compared to both a high quality Monte Carlo simulation and an analytically determined pdf.

While the analytical pdf has qualitative agreement with the truth, it fails to reproduce the magnitude of the long left tail due to very tight tuning requirements. In comparison, after just 60 experiments the left tail has been matched in both shape and magnitude.

In figure 4, the l_2 error in the recovered pdf and recovered mapping is shown for three sampling methods: Q-criterion active search, (fixed) Latin hypercube sampling (LHS), and simple Monte Carlo (MC) sampling. While both Q-criterion and LHS significantly outperform MC, there is little difference between LHS and Q-criterion sampling on the l_2 error. This is because, as previously noted, l_2 error preferentially weighs the mode of the distribution relative to the tails.

In figure 5, we compare the tail mass of the recovered pdf from each sampling methods. Immediately, we note that MC sampling completely fails to identify the long the tails at all. Q-criterion

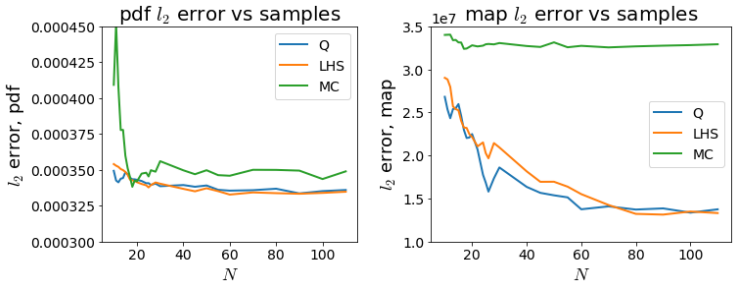

Fig. 4: l_2 error of a) the recovered pdf and b) the recovered mapping. Note that l_2 error of the pdf is a very poor error metric, because it ignores the long tail.

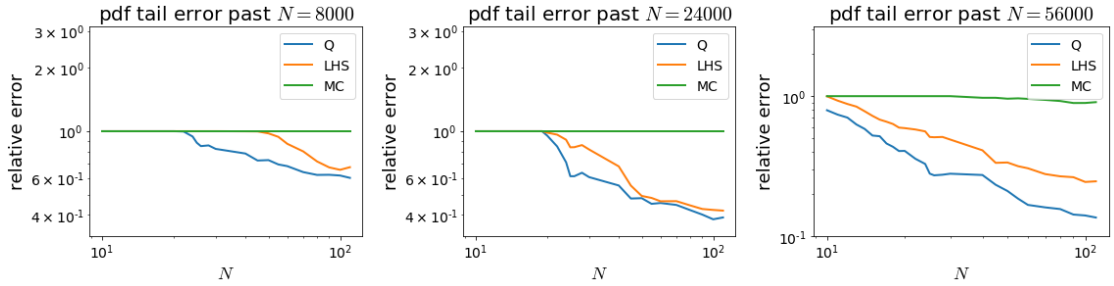

Fig. 5: Error in the recovered pdf tail mass, for three different thresholds a) $N = 8000$, b) $N = 24000$, c) $N = 56000$. Note that while both Latin hypercube sampling (LHS) and Q-criterion active search outperform simple random samples, active search generally outperforms LHS in the region of interest ($20 < N < 100$ samples).

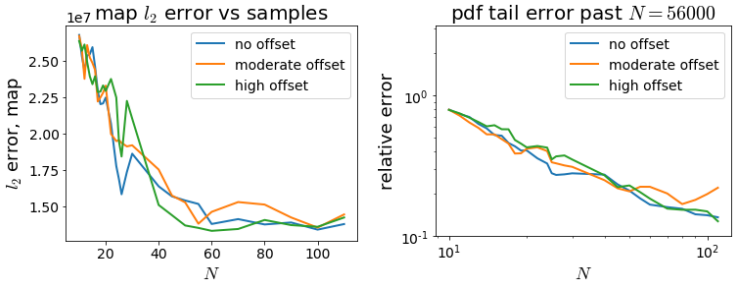

Fig. 6: Comparison of the recovered 1) map and b) tail error for different choices of the GMM fitting offset. Dependence on the zero value for GMM fitting was nearly nonexistent.

active search slightly outperforms fixed LHS, though the size of the gap changes depending on the particular long-tail cutoff and number of samples.

We previously hypothesized that the broad plateau region of the true map (see figure 3) might cause problems for the GMM fitting. Indeed, there are occasional fitting outliers in the $10 < N < 20$ region where the Q criterion significantly overestimates the tail mass of the recovered pdf (not shown).

To test this, we ran the Q criterion active search with three different fitting step offsets: $\bar{n} = 0$, $\bar{n} = 71,000$, and $\bar{n} = 40,000$. These choices represent no offset, the approximate distribution mode, and a compromise midpoint. Figure 6 shows the l_2 map error and tail error associated with each offset. it is clear that while the fitting offset changes the exact surrogate GMM fit, the output pdf tails are relatively insensitive to the details of the surrogate fitting.

Future work should be done to investigate the balance between more powerful models (GMM with more radial basis functions) and numerical instability during the fitting step.

4 Conclusion

We showed that rainflow counting disagrees with direct integration when predicting material fatigue failure in the presence of intermittent loads. In particular, we showed that rainflow counting substantially underestimates both the variance of N_{fail}, and the probability of extreme leftward deviations–the long tail.

On the other hand, we showed that an analytic algorithm based on domain decomposition had similar computational advantages but substantially less accuracy loss. In particular, the analytic algorithm captured the long tail caused by intermittent spikes in the loading signal.

Additionally, we used an active search package to learn a function mapping parametrized load signals into predicted failure times. This active search approach required only a small number of (numerical) experiments, and did not require prior knowledge of the material coherent envelope. While the results of this experimental design do not exactly reproduce the correct pdf, they do capture the long tail using significantly fewer experiments than traditional Monte Carlo approaches.

In the future, this approach should be extended to more complicated structures consisting of multiple finite elements. This extension will require more complicated input space parametrizations, but it would allow calculating the fatigue lifetime of real structures, such as oil risers and wind turbines, in the presence of intermittent loading with known distributions.

References

1. *Dynamic Response and Fatigue Reliability Analysis of Marine Riser Under Random Loads*, volume Volume 2: Structures, Safety and Reliability; Petroleum Technology Symposium of *International Conference on Offshore Mechanics and Arctic Engineering*, 06 2007.
2. *Exploring and Exploiting a Surrogate*, chapter 3, pages 77–107. John Wiley & Sons, Ltd, 2008.
3. Antoine Blanchard and Themistoklis P. Sapsis. Output-weighted importance sampling for bayesian experimental design and rare-event quantification. *Manuscript in preparation.*
4. Antoine Blanchard and Themistoklis P. Sapsis. Bayesian optimization with output-weighted importance sampling. *Submitted to Journal of Computational Physics*, 2020.
5. Kathryn Chaloner and Isabella Verdinelli. Bayesian experimental design: A review. *Statistical Science*, 10(3):273–304, 1995.

6. K.R. Chernyshov. Information-theoretic statistical linearization. *International Federation of Automatic Control*, 49(12), 2016.
7. M. Ciavarella, P. D'antuono, and A. Papangelo. On the connection between palmgren-miner rule and crack propagation laws. *Fatigue & Fracture of Engineering Materials & Structures*, 41(7):1469–1475, 2018.
8. Tatsuo Endo, Koichi Mitsunaga, Kiyohumi Takahashi, Kakuichi Kobayashi, and Masanori Matsuishi. Damage evaluation of metals for random or varying loading. three aspects of rain flow method. *Proceedings of the 1974 Symposium on Mechanical Behavior of Materials*, pages 371–380, 1974.
9. Yong Gyo Lee, Xavier Garza-Gomez, and Rose M. Lee. Ultimate costs of the disaster: Seven years after the deepwater horizon oil spill. *Journal of Corporate Accounting & Finance*, 29(1):69–79, 2018.
10. Weifei Hu, K. K. Choi, Olesya Zhupanska, and James H.J. Buchholz. Integrating variable wind load, aerodynamic, and structural analyses towards accurate fatigue life prediction in composite wind turbine blades. *Struct. Multidiscip. Optim.*, 53(3):375–394, March 2016.
11. Xun Huan and Youssef M. Marzouk. Simulation-based optimal bayesian experimental design for nonlinear systems. *Journal of Computational Physics*, 232:288–317, 2013.
12. S. Serebrinsky I. Arias and M. Ortiz. A phenomenological cohesive model of ferroelectric fatigue. *Acta Materialia*, 54:975–984, 2006.
13. Shali Jiang, Gustavo Malkomes, Geoff Converse, Alyssa Shofner, Benjamin Moseley, and Roman Garnett. Efficient nonmyopic active search. In *Proceedings of the 34th International Conference on Machine Learning - Volume 70*, ICML'17, page 1714–1723. JMLR.org, 2017.
14. Han Kyul Joo, Mustafa A. Mohamad, and Themistoklis P. Sapsis. Heavy-Tailed Response of Structural Systems Subjected to Stochastic Excitation Containing Extreme Forcing Events. *Journal of Computational and Nonlinear Dynamics*, 13(9), 07 2018. 090914.
15. Gustavo Malkomes, Chip Schaff, and Roman Garnett. Bayesian optimization for automated model selection. In Frank Hutter, Lars Kotthoff, and Joaquin Vanschoren, editors, *Proceedings of the 2016 Workshop on Automatic Machine Learning, AutoML 2016, co-located with 33rd International Conference on Machine Learning (ICML 2016), New York City, NY, USA, June 24, 2016*, volume 64 of *JMLR Workshop and Conference Proceedings*, pages 41–47. JMLR.org, 2016.
16. Mustafa A. Mohamad and Themistoklis P. Sapsis. Probabilistic description of extreme events in intermittently unstable dynamical systems excited by correlated stochastic processes. *SIAM/ASA J. Uncertainty Quantification*, 3:709–736, 8 2015.
17. M. Murata, H. Nagano, and K. Kashino. Unscented statistical linearization and robustified kalman filter for nonlinear systems with parameter uncertainties. In *2014 American Control Conference*, pages 5079–5084, June 2014.
18. Will Cousins Mustafa A. Mohamad and Themistoklis P. Sapsis. A probabilistic decomposition-synthesis method for the quantification of rare events due to internal instabilities. *Journal of Computational Physics*, 322:288–308, 6 2016.
19. A. Olsson, G. Sandberg, and O. Dahlblom. On latin hypercube sampling for structural reliability analysis. *Structural Safety*, 25(1):47 – 68, 2003.
20. Themistoklis P. Sapsis. Output-weighted optimal sampling for bayesian regression and rare event statistics using few samples. *Proceedings of the Royal Society A*, page 476, 2020.
21. S. Serebrinsky and M. Ortiz. A hysteretic cohesive-law model of fatigue-crack nucleation. *Scripta Materialia*, 53(1):1193–1196, 2005.
22. P.D. Spanos and I.A. Kougioumtzoglou. Harmonic wavelets based statistical linearization for response evolutionary power spectrum determination. *Probabilistic Engineering Mechanics*, 27(1):57 – 68, 2012. The IUTAM Symposium on Nonlinear Stochastic Dynamics and Control.
23. Ky Khac Vu, Claudia D'Ambrosio, Youssef Hamadi, and Leo Liberti. Surrogate-based methods for black-box optimization. *International Transactions in Operational Research*, 24(3):393–424, 2017.
24. Peter Wolfsteiner. Fatigue assessment of non-stationary random vibrations by using decomposition in gaussian portions. *International Journal Mechanical Sciences*, 127, 2017.

25. Ruoxue Zhang and Sankaran Mahadevan. Fatigue reliability analysis using nondestructive inspection. *J. Strct. Eng.*, 128(8), 2001.
26. E. Zio and N Pedroni. Estimation of the functional failure probability of a thermal-hydraulic passive system by subset simulation. *Nuclear Engineering and Design*, 239:580–599, 10 2008.